Dihydrogen Bonding in Main Group Elements: An ab Initio Study

Sudhir A. Kulkarni*,†

Department of Chemistry, University of Pune, Pune 411 007, India

Received: April 7, 1998; In Final Form: June 5, 1998

The occurrence of dihydrogen bonds in the complexes and dimers of complexes involving the main group elements is systematically investigated. The complexes of LiH, BH_3, and AlH_3 with HF, H_2O, and NH_3 as well as dimers of these complexes are studied using ab initio calculations at the MP2 level. The complexes having H···H bonding are observed; however, in most of the cases they are not minima on their PES. The $[H_2OLiH]_2$ has a compact C_{2h} structure with a large dimerization energy where the H···H bond exhibits features of a hydrogen bridge. The H···H bond energy in $[BH_3HF]_2$, $[BH_3H_2O]_2$, and $[AlH_3H_2O]_2$ is analogous to the conventional moderate or weak hydrogen bond. The bonding features of these complexes and their dimers are analyzed using electron density topography. The structures of dimers are rationalized using molecular electrostatic potential maps. The decomposition analysis of interaction energies of dimers reveals the predominance of electrostatic contribution followed by charge transfer and polarization.

I. Introduction

Recent theoretical and experimental studies on transition metal complexes involving a new type of interaction EH···HX (where E is transition/alkali metal or boron and X is any electronegative atom/group) have stimulated a lot of interest.[1] A new term, viz., the "dihydrogen bond" has been coined by Richardson et al.[1] to describe this novel bond. The H···H contact distances and heats of interaction for these systems lie within the range of the conventional H-bonds, viz., 1.6−2.2 Å and 3−8 kcal/mol, respectively. Moreover, in transition metal complexes, both inter- as well as intramolecular versions of the dihydrogen bond have also been observed.[2,3] It has been proposed that these bonding features may be used in selectively stabilizing transition states, thereby leading to increase in reaction rates,[1] making them potential catalytic agents.

Several theoretical studies on the dihydrogen-bonded metal complexes investigating various factors responsible for bonding have been carried out.[1−6] On the other hand, there have been few attempts reported in the literature to investigate dihydrogen bonding exhibited by the main group elements. Liu and Hoffmann[5] explored the possibility of H···H bonding in the LiH···HF complex at the RHF and MP2 levels and found that such bonding is not possible owing to high exothermicity of the reaction LiH + HF → LiF + H_2. Richardson et al.[1] have theoretically investigated the H···H bonding in BH_3NH_3. Although the H···H bonding has not been observed in the parent complex, it manifests itself in the dimer of BH_3NH_3 in a head-to-tail fashion. The resultant dimer structure is cyclic and of C_2 symmetry with two dihydrogen bonds. The density functional (B3LYP) estimates of the H···H distance and interaction energy turn out to be 1.8 Å and 12.1 kcal/mol, respectively. The Cambridge Crystallographic database showed 18 amine−borane structures[1] with short H···H bonds in the range of 1.7−2.2 Å and strongly bent B−H···(HN) angles in the range of 95−120°, whereas the N−H···(HB) angles were found to lie in the range of 160−180°. The ab initio structure of the BH_3NH_3 dimer verifies and supports the strongly bent angles[1] of dihydrogen bonding. A comparative study of $[BH_3NH_3]_2$, $[AlH_3NH_3]_2$, and $[GaH_3NH_3]_2$ at the B3LYP as well as MP2 levels has recently been reported.[6] The $[BH_3NH_3]_2$ was found to be of C_{2h} symmetry, whereas the other dimers have a C_2 symmetry. Further, the dimerization energies are found to decrease from boron to gallium in this series.

The purpose of the present study is to systematically investigate the occurrence of dihydrogen bonds in the complexes involving the main group elements. The structures having close H···H bonds in the complexes of LiH, BH_3, and AlH_3 with HF, H_2O, and NH_3 are studied. In addition, the structures of dimers of these complexes are obtained to verify the existence of the dihydrogen bond. The factors responsible for the formation of the dihydrogen bond in the parent complexes and the corresponding dimers are discussed. The bonding in these complexes and their dimers has been compared on the basis of interaction energies as well as topological analysis of their electron densities. It has been remarked in the earlier studies that the H···H interaction is mainly electrostatic in nature,[1] a verification of which is also taken up in the present study. The methodology used herein is discussed in section II, while the structure and energetics of complexes of LiH, BH_3, and AlH_3 are described in the sections III.A−III.C, respectively. Section IV investigates the electron density topography of the complexes and dimers as well as their molecular electrostatic potentials. Section V reports their energy decomposition, followed by concluding remarks in section VI.

II. Methodology

The structures of the complexes and their dimers studied herein are obtained using the restricted Hartree−Fock (RHF/6-31++G(d,p)) and Moller−Plesset perturbation methods (MP2/6-31++G(d,p)) from the program GAMESS.[7] The basis set used is of split-valence type including diffuse functions on all the atoms with polarization functions on hydrogens as well as heavy atoms. The nature of stationary points obtained is confirmed by calculating their vibrational frequencies at the MP2/6-31++G(d,p) level. It has been observed that structural parameters of several dihydrogen-bonded complexes at the MP2

† E-mail: sakul@chem.unipune.ernet.in.

S1089-5639(98)01763-0 CCC: $15.00
Published on Web 09/02/1998

level are comparable to those predicted by the B3LYP density functional method.[6,8] The MP2 geometries are used for calculating interaction energies with the coupled cluster method including singles, doubles, and noniterative triples contributions (CCSD(T)/6-31++G(d,p)) for some complexes and dimers using the program Gaussian 94.[9] The topographical analysis of the electron density distribution of all the systems studied here is performed to understand clearly the bonding features of the dihydrogen-bonded dimers and their parent complexes using the program UNIPROP.[10] The molecular electrostatic potential (MESP) of the complexes is utilized for rationalizing the structures of the dimers. The MESP-derived charges have also been used in some cases. The visualization of MESP isosurfaces have been done by using the program UNIVIS.[10] The energy decomposition analysis due to Kitaura and Morokuma[11] is performed for the dihydrogen-bonded complexes and/or their dimers.

III. Results and Discussion

The systems studied here are essentially simple molecular complexes capable of forming a dihydrogen bond. The hydrides of lithium, boron, and aluminum have negatively charged hydrogens, whereas NH_3, H_2O, and HF possess positively charged hydrogens. The simple Mulliken charges of the isolated complexing molecules are given below:

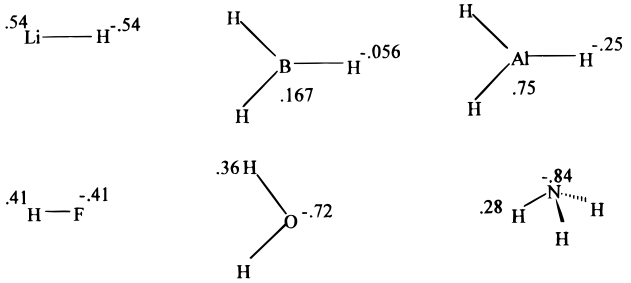

The formation of dimers of the complexes may be rationalized using these Mulliken charges. In the present study, we explore the structures that are expected to engender the H···H bond in addition to some other reported structures.[4,12] The interaction energies and geometrical parameters reported in the following discussion are computed at the MP2 level, unless mentioned otherwise.

III. A. Complexes of LiH. The complexes of LiH with HF have already been studied earlier,[4,5] and there are reports on comparison of the interaction energies of LiH···HF and HNO···HF at the RHF/6-31G* level.[4] Although the H···H bonding is observed at the RHF level for LiH···HF, there is no stationary structure exhibiting such a bond at the MP2 level. Thus, the dihydrogen-bonded structure for LiH···HF may be regarded as an artifact of the HF theory, and the inclusion of electron correlation seems to be vital for validation of the dihydrogen bonding.

The structures of three stationary points on the potential energy surface (PES) of LiH···H_2O are shown as S_1, S_2, and S_3 in the Figure 1 with their interaction energies at the RHF, MP2, and CCSD(T) level reported in Table 1. In S_1 and S_2, Li and O are bonded and these structures are minima on the PES. The structure S_2 has close contacts between Li and O as well as H and H and has a stabilization comparable to S_1 (cf. ZPE-included interaction energies in Table 1). Interestingly, a structure analogous to S_2 does not exist on the RHF level PES. Further, a bidentate structure S_3 with a stabilization energy of −5.51 kcal/mol has two imaginary frequencies and hence not

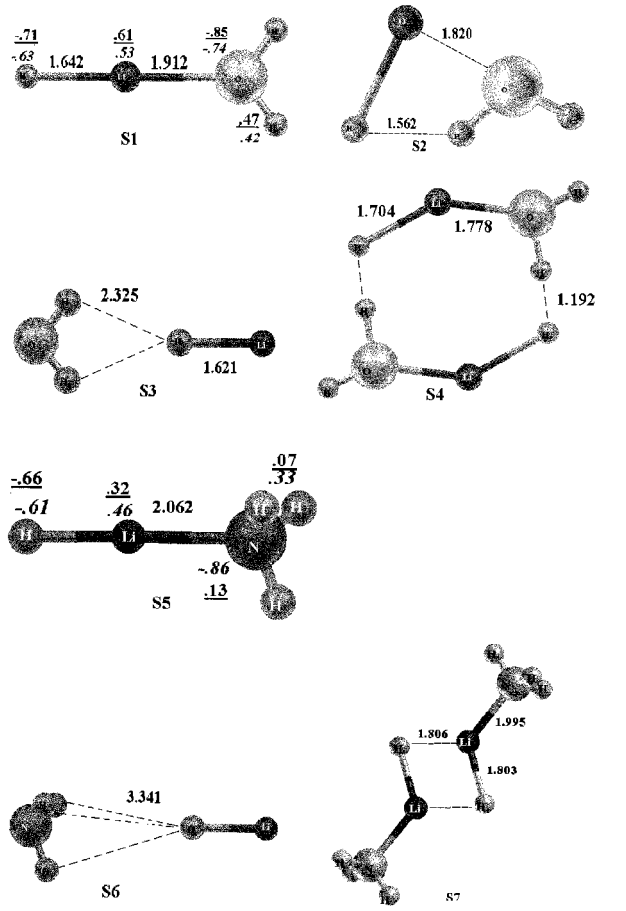

Figure 1. Stationary structures of complexes of LiH with H_2O and NH_3 and dimers of complexes. Bond lengths are in Å. Mulliken charges for some complexes are shown in italics, whereas MESP-driven charges are underlined.

been analyzed further. The Mulliken charges of S_1 when compared with LiH and H_2O charges reveal that the hydride of lithium has acquired higher negative charge, whereas the hydrogens in H_2O exhibit a higher positive charge in the complex S_1. Similar trends are shown by MESP-derived charges shown in Figure 1. This clearly indicates that the dimer of this complex is a promising candidate for H···H bonding. Further, the dipole moment of S_1 is very high (cf. Table 1).

The dimer of LiH···H_2O (cf. S_4 in Figure 1) exhibits a cyclic eight-membered structure with two close H···H bonds of 1.192 Å. The structure bears C_{2h} symmetry and is a minimum on the PES. The angle (O)H···H−Li is strongly bent (113.3°), whereas (Li)H···H−O angle is 176.8° (the angle (O)H···H−Li indicates an angle between vectors H···H and H−Li). This structure is stabilized by −45.34 and −40.01 kcal/mol at the MP2 and CCSD(T) levels, respectively, and therefore can be termed as a strong dihydrogen bond. The high stabilization energy in the range of 14−40 kcal/mol has been reported[13] for the conventional strong hydrogen-bonded systems, such as FHF^- involving ionic configuration. As seen earlier, in LiH···H_2O (S_1), the LiH hydrogen acquires more negative charge, which is reflected in its dipole moment (cf. Table 1), and head-to-tail interaction of two such complexes cooperatively leads to high stabilization. The high stability may also be attributed to large structural deformations and a very short H···H bond, which can be considered as a hydrogen bridge. The overlap population analysis shows population of 0.512 and bond order of 0.651 for the H···H bond. Further, the 2p population of hydrogen

TABLE 1: Interaction Energies (kcal/mol) and Dipole Moment μ (Debye) of Complexes of LiH, BH_3, and AlH_3 with HF, H_2O, and NH_3 Using the 6-31++G(d,p) Basis Set[a]

structure	NIMAG[b]	ΔE(RHF)	ΔE(MP2)	ΔE(MP2)+ZPE	ΔE(CCSDT)+ZPE	μ[c]
S_1	0	−19.60	−20.23	−18.15	−17.57	9.01
S_2	0		−20.71	−18.27	−15.24	
S_3	2	−4.60	−5.51	−4.34		
S_5	0	−22.24	−23.58	−21.19	−20.73	8.81
S_6	2	−1.17	−1.46	−1.01		
S_8	0	−1.51	1.47	3.52	−1.16	
S_9	1	−0.62	−1.13	−0.42		
S_{10}	1	−0.86	−1.53	−0.55		
S_{12}	0	−6.44	−14.26	−9.35	−8.85	2.29
S_{13}	0	−0.44	−0.98	0.12	0.14	
S_{14}	1	−0.36	−0.73	−0.23		
S_{16}	1	−2.37	−3.50	−2.32		
S_{17}	2	−0.53	−1.01	−0.36		
S_{18}	1	−6.71	−8.90	−6.91		
S_{19}	0	−7.02	−9.27	−7.03	−6.58	2.96
S_{20}	1	−1.19	−2.02	−0.84		
S_{21}	0	−17.78	−11.86	−8.63	−16.89	4.75
S_{23}	0	−26.55	−20.95	−17.39	−25.96	5.49

[a] Total energies (in au) of complexing molecules at RHF, MP2, and CCSD(T) levels are LiH, −7.982 62, −8.003 52, −8.009 60; BH_3, −26.393 54, −26.492 13, −26.509 87; AlH_3, −243.620 60, −243.702 57, −243.713 68; HF, −100.024 31, −100.218 29, −100.221 69; H_2O, −76.031 31, −76.236 21, −76.244 68; NH_3, −56.201 15, −56.396 33, −56.411 09. [b] Number of imaginary frequencies. [c] Dipole moments calculated at the MP2 level.

attached to the oxygen increases significantly in a dimer, which explains the strong bent structure of the dihydrogen bond.

There are two stationary structures on the PES of LiH···NH_3 shown as S_5 and S_6 in Figure 1. The S_5 has a C_{3v} symmetry and possesses a N···Li bond and has been reported earlier in the literature.[12] The stabilization of this complex is about −21 kcal/mol at both MP2 and CCSD(T) levels. The Li−H bond has elongated by 0.02 Å in the complex S_5. The Mulliken charges show a comparatively higher negative charge on the hydrogen of the LiH fraction and higher positive charge on the hydrogens of NH_3 in the complex S_5. However, the MESP-derived charges of S_5 are strikingly different from the Mulliken charges. The complex S_6 has a tridentate structure with a long H···H bond and a stabilization of −1.46 kcal/mol. However, this structure is not a minimum on the PES.

Although the Mulliken charges of S_5 suggest that the dimerization of the complex LiH···NH_3 is favorable, the dihydrogen-bonded structure has not actually been observed. The dimerization of S_5 leads to the structure S_7, which has two LiH···LiH bonds as shown in Figure 1 and has an interaction energy of −40.10 kcal/mol. The MESP-derived charges (cf. Figure 1) show that the difference between the charges on NH_3 hydrogens and hydride in S_5 is more than that in LiH···H_2O complex (S_1), leading to attraction of the hydride by lithium of the other complex in S_7.

III. B. Complexes of BH_3. The complexation of BH_3 with HF yields three stationary structures S_8, S_9, and S_{10} as depicted in Figure 2. The S_8 is the conventional structure with a weak bonding between B and F and is a minimum on the PES. There is an increase in the negative charge of two hydrogens attached to boron and an increase in the positive charge of hydrogen in the HF part in S_8 favoring the dihydrogen-bonded dimer structure. Although the S_9 and S_{10}, respectively, have monodentate and bidentate H···H-bonded structures, they are not minima on the PES. Further, the distance between H···H exceeds 2.2 Å in S_9 and S_{10}, and hence they have small stabilization energies. The cyclic dimer of S_8 also forms an eight-membered structure of C_{2h} symmetry with the H···H bond as short as 1.382 Å (cf. S_{11} in Figure 2). The ZPE-corrected stabilization energy is −4.85 kcal/mol at the MP2 level and −4.69 kcal/mol at the CCSD(T) level. Thus, the stabilization

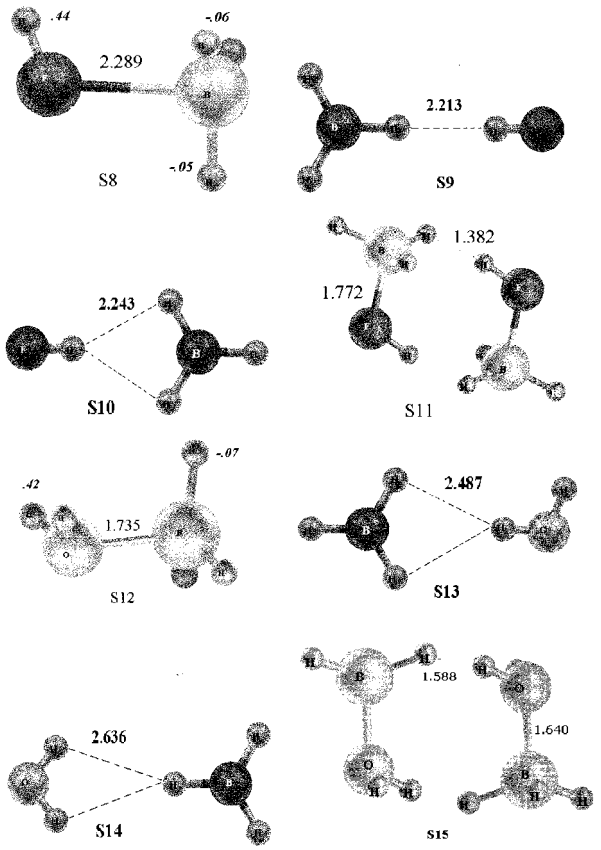

Figure 2. Stationary structures of complexes of BH_3 with HF and H_2O and dimers of complexes. Bond lengths are in Å. The Mulliken charges for some complexes are shown in italics.

due to each H···H bond is estimated to be −2.4 kcal/mol. The weak stabilization for such a short H···H bond may be attributed to the increased nuclear repulsion (steric interaction) due to compact ring formation. This is clearly observable from the short B−F bond in the dimer (1.772 Å) compared to that in the complex (2.301 Å). The angles (F)H···H−B and F−H···H(B) are 106.8 and 165.9° respectively, indicating that the former is a bent bond whereas the latter is analogous to conventional H-bond.

Three stationary structures are found on the PES of $BH_3\cdots H_2O$. The S_{12} complex has a B···O bond of length 1.735 Å and is stabilized by −9.35 kcal/mol. The complex shows an enhancement in the negative charge on the hydrogens attached to boron and positive charge on the hydrogens of H_2O. This situation is clearly favorable for the dimer formation analogous to the BH_3HF case. Among other structures, the S_{13} is a minimum on the PES and has a bidentate planar structure wherein two hydrogens of BH_3 are bonded to one hydrogen of H_2O. However, the interaction energies obtained at the MP2 and CCSD(T) levels show that this structure is not a stable one. The S_{14} is also a planar, bidentate structure with one of the hydrogens of BH_3 symmetrically bonded to two hydrogens of water at a distance of 2.636 Å. This structure is also not a minimum on the PES. A dimer of BH_3H_2O is observed to form two dihydrogen bonds leading to an eight-membered cyclic structure with a C_{2h} symmetry (cf. S_{15} in Figure 2). The contact distance between the H···H is 1.588 Å resulting into the stabilization of 13.06 kcal/mol. The B···O bond in the dimer is shorter by 0.095 Å than that in the complex. On the other hand, the B−H and O−H bonds involved in H···H bonding are elongated by 0.022 and 0.019 Å, respectively, in the dimer compared to those in the complex. The angles (O)−H···H−B and (B)−H···H−O are found to be 103.5 and 161.8°, respectively. Since, the structural changes in the dimer geometry of the complex BH_3H_2O are small, the energy of each dihydrogen bond is about 6.5 kcal/mol.

The results of the dimer of BH_3NH_3 reported earlier[1,6] and the present results for $[BH_3H_2O]_2$ and $[BH_3HF]_2$ clearly indicate that one of the angles (X)H···H−E involved in dihydrogen bonding is strongly bent whereas the other angle X−H···H(E) is almost linear analogous to the conventional hydrogen bond. The 2p population of hydrogens attached to fluorine or oxygen in $[BH_3HF]_2$ and $[BH_3H_2O]_2$ has increased; this provides the possibility of a bent H···H bond in the dimer structures. Such bent B−H···H(N) angles have been observed in several structures obtained from Cambridge Crystallographic Database.[1] The structure of $[BH_3NH_3]_2$ has not been calculated at the MP2 level in the present investigation. It has been revealed in earlier studies[6] that B3LYP structures and dimerization energies are comparable to MP2 ones. To verify the fact that structures obtained by the MP2 and B3LYP levels are quite close to each other, we have optimized the structures of BH_3, H_2O, BH_3H_2O (S_{12}), and $[BH_3H_2O]_2$ (S_{15}) at the B3LYP/6-31++G(d,p) level. At the B3LYP level, the B···O bond in the complex BH_3H_2O is longer by 0.004 Å and interaction energy is about 1.0 kcal/mol higher than the corresponding MP2 value. Although the dihydrogen bond is shorter by 0.067 Å for the $[BH_3H_2O]_2$ at the B3LYP level, the dimerization energy is −17.27 kcal/mol, which exactly matches the corresponding MP2 estimate. The angles (O)−H···H−B and (B)−H···H−O are 105.2 and 164.3° at the B3LYP level showing that there is a clear-cut trend in the bending of (X)H···H−B angle: bending decreases as the electronegativity of the element X increases, a trend also followed by the MP2 geometries. Hence it is felt that this level of calculations should be sufficient for the present study.

III. C. Complexes of AlH_3. AlH_3 has many features analogous to BH_3 and hence is a good candidate for the study of the effect of change in the period of the element. As intuitively expected, the Mulliken charges of AlH_3 show that hydrogens are more negative than those in the BH_3. We therefore study the effect of increased charge of hydrogens on the structures of the complexes with HF, H_2O, NH_3, and their corresponding dimers.

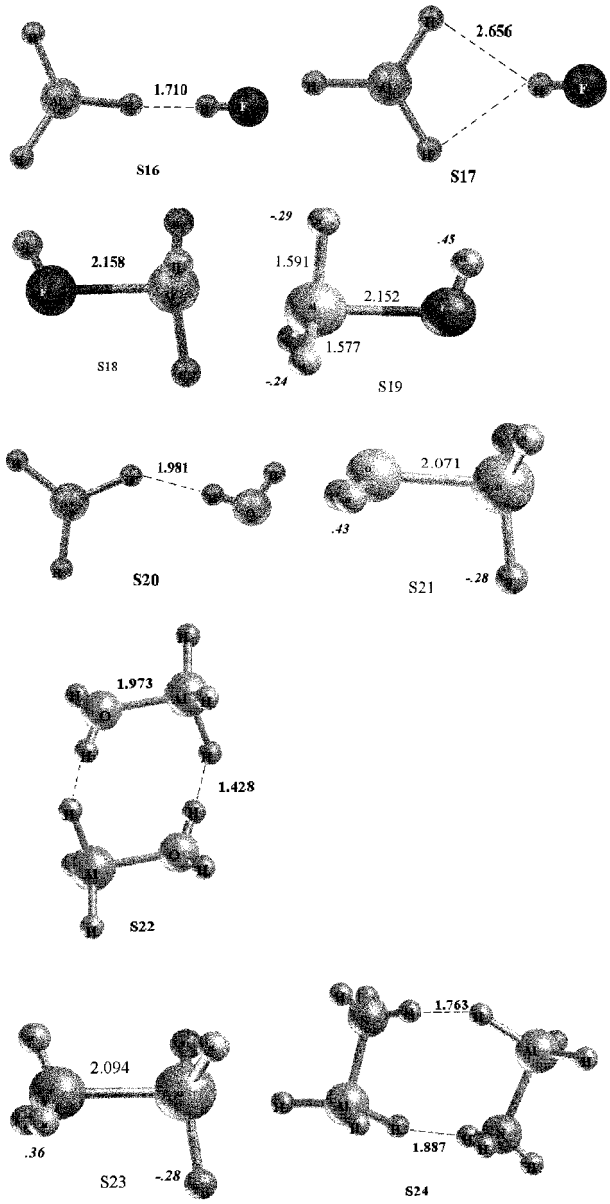

Figure 3. Stationary structures of complexes of AlH_3 with HF, H_2O, and NH_3 and dimers of complexes. Bond lengths are in Å. The Mulliken charges for some complexes are shown in italics.

There are four structures of the complex $AlH_3\cdots HF$, which are shown as (S_{16}−S_{19}) in Figure 3. The S_{16} is a monodentate structure with the H···H bonding of 1.71 Å and stabilization of −2.32 kcal/mol. The S_{17} is a bidentate structure involving two hydrogens of AlH_3 and a weakly bonded hydrogen of HF at a distance of 2.656 Å with a small interaction energy (−1.01 kcal/mol). The structure S_{18} has an Al···F bond of length 2.158 Å and has a dihedral angle H−Al−F−H of 180°. This structure has the interaction energy of −6.91 kcal/mol. However, structures S_{16}−S_{18} are not minima on the PES. The S_{19} also exhibits Al···F bonding but has a H−Al−F−H dihedral angle of 0° and is a minimum on the PES with an interaction energy of −7.03 kcal/mol with the Al−F and (Al)H···H(F) distances of 2.152 and 2.454 Å, respectively. One of the hydrogens of AlH_3 acquires a more negative charge, whereas the hydrogen attached to fluorine gets a more positive charge in S_{19}. Instead of formation of a dihydrogen-bonded dimer of AlH_3HF, it leads to the formation of $AlH_2F + H_2$. The energy for this reaction at the MP2 level is −26.31 kcal/mol.

The $AlH_3\cdots H_2O$ complexes are shown as structures S_{20} and S_{21} in Figure 3. The structure S_{20} is a planar one with a H···H bond of length 1.981 Å. This complex is also not a minimum on the PES and has small a stabilization energy. The structure S_{21} has an Al···O bond of length 2.058 Å and is a minimum on the PES with an interaction energy of −8.63 kcal/mol. The Mulliken charges of S_{21} show a pattern similar to those of the $BH_3\cdots H_2O$ complex (S_{12}), i.e., the hydrogens attached to Al acquire more negative charge whereas the hydrogens of H_2O acquire more positive charge. The complex structure seems to be favorable for the dimer formation.

The dimer of $AlH_3\cdots H_2O$ is indeed observed (cf. S_{22} in Figure 3) to have a cyclic C_{2h} structure analogous to the dimer of $BH_3\cdots H_2O$. However, the interaction energy of $[AlH_3H_2O]_2$ is more by −3.22 kcal/mol compared to that of $[BH_3H_2O]_2$ as the H···H bond is closer by 0.16 Å in the former. The Al−O bond is shortened by 0.1 Å in the dimer compared to that in the complex S_{20}. The angles (Al)H···H−O and (O)H···H−Al are 174.7° and 123.3°, respectively. The shorter dihydrogen bonds and greater interaction energy may be attributed to the higher negative charge of the hydrogens of AlH_3.

The complex of AlH_3 with NH_3 is depicted as structure S_{23} in Figure 3. The S_{23} has an Al···N bond length of 2.094 Å and is stabilized by −17.39 kcal/mol. The Mulliken charges of the complex show an increase in the negative charge of hydrides of Al as well as an increase in positive charge of hydrogens in NH_3. This indicates the possible formation of the AlH_3NH_3 dimer. When calculations for other H···H bonded complexes were performed, no structure with significant stabilization energy was found.

The dimer of AlH_3NH_3 has a peculiar cyclic structure (cf. Structure S_{24}) with two dihydrogen bonds of different lengths between two monomer complexes. One of the H···H bonds is monodentate of length 1.763 Å, while the other is bifurcated with the length of 1.887 Å. The Al···N distance is shorter by 0.04 Å in the dimer than in the complex. The angles (Al)H···H−N are 165.3° and 170.9° whereas the angles (N)H···H−Al are 110.3° and 131.0° for the bifurcated and monodentate bonds, respectively. The interaction energy of the dimer compared to monomer is −11.36 kcal/mol. Since the dihydrogen bonds are dissymmetric, the energy of each H···H bond would be different. The geometry optimization at the B3LYP/6-31++G(d,p) level for $[AlH_3NH_3]_2$ shows a C_2 symmetry for the dimer, similar to that in the earlier reports[6] with a dimerization energy of −12.14 kcal/mol. The MP2 and CCSD(T) calculations at the B3LYP optimized geometry show that they are 0.43 and 0.48 kcal/mol higher in energy than the corresponding MP2-optimized one. This probably indicates that geometry of this dimer is highly sensitive to basis set and level of calculation.

Table 1 also reports dipole moments of complexes forming dihydrogen-bonded dimers. The dipole moment of the H_2OLiH complex is highest, whereas that of BH_3HF is lowest. The dimerization energies of these complexes also show trends similar to that shown by dipole moments of the complexes. The dipole moments of dimers are zero except for $[AlH_3NH_3]_2$, which has dipole moment of 0.98 D.

The effect of basis set superposition error[14] (BSSE) estimates deserves a special mention in the present study. The computation of BSSE for the H···H-bonded dimers show that $[H_2OLiH]_2$, $[BH_3HF]_2$, and $[BH_3H_2O]_2$ have corrections of −20.77, −7.32, and −10.54 kcal/mol, respectively. The large stabilization after inclusion of BSSE may be attributed to significant geometrical distortions in the monomer complexes in their dimer geometries compared to their equilibrium structures. Thus, the use of dimerization energies without inclusion of BSSE is recommended for H···H bonding.

TABLE 2: Dimerization Energies (kcal/mol) of Complexes Involving Dihydrogen Bonds

structure	ΔE(RHF)	ΔE(MP2)	ΔE(MP2)+ZPE	ΔE(CCSDT)+ZPE
$[H_2OLiH]_2$	−33.90	−46.61	−45.34	−40.01
$[BH_3H_2O]_2$	−10.35	−17.26	−15.51	−13.06
$[BH_3HF]_2$	−4.96	−10.04	−4.85	−4.69
$[AlH_3NH_3]_2$	−9.51	−13.18	−11.36	−9.44
$[AlH_3H_2O]_2$	−14.48	−20.48	−18.42	−16.52

[a] Total energies (in au) of complexes at RHF, MP2, and CCSD(T) levels are H_2OLiH, −84.045 10, −84.271 97, −84.285 59; BH_3H_2O, −102.435 11, −102.751 07, −102.776 48; BH_3HF, −126.420 26, −126.708 07, −126.736 68; AlH_3NH_3, −299.864 06, −300.132 29, −300.171 82; AlH_3H_2O, −319.680 25, −319.957 68, −319.990 43.

IV. Bonding Features via Electron Density and Electrostatic Potential

For achieving detailed information on the bonding features of the complexes leading to dihydrogen-bonded dimers and the corresponding dimers, topological analysis of electron density (ED) is performed. The topological analysis involves location and characterization of the critical points (CP) in ED distribution and their chemical interpretation.[15] The ED and Laplacian of ED and bond ellipticity at bond CP are the parameters used for the analysis. The negative Laplacian is an indicator of a covalent bond whereas the positive Laplacian indicates nonbonding or closed-shell interaction between the two atoms.[16] The bond ellipticity defined from eigenvalues λ_I of the Hessian matrix of ED as $\epsilon = \lambda_1/\lambda_2 - 1$, where λ_1 and λ_2 are magnitudes of negative eigenvalues with $|\lambda_1| > |\lambda_2|$, is an indicator of extent of double-bond character. In addition, the bond ellipticity provide a measure structural stability; the bonds with large ϵ values are prone to rupture.[17] These parameters are to be compared among complexing molecules, complexes, and dimers of complexes discussed in the previous section. It is well-known that the conventional hydrogen bonds have a positive Laplacian at the bond critical point (BCP),[18] and topological analysis of dihydrogen bonding in $[BH_3NH_3]_2$ has been investigated recently.[19] Table 3 provides the topological analysis of the ED distributions at the MP2/6-31++G(d,p) geometries.

The H_2OLiH complex S_1 shows a weak bond between Li and O, which also exhibits noncovalent interaction as shown by a positive Laplacian value. In dimer of H_2OLiH the LiO bond has greater ED at the BCP, whereas Li−H and O−H bonds involved in the dihydrogen bonding have reduced ED at their BCPs compared to the complex. The BCP corresponding to the dihydrogen bond has substantial electron density and, more interestingly, a negative Laplacian, supporting the formation of a hydrogen bridge in the dimer as discussed earlier.

The complex BH_3HF shows a weak B−F bond as seen from the higher ellipticity (cf. Table 3), and one of the B−H shows greater ED at the BCP. In the $[BH_3HF]_2$, the B−F bond has greater ED as reflected from smaller bond length compared to that in the complex. The H−F as well as B−H bonds involved in the dihydrogen bonding become weaker owing to sharing of ED in the H···H bond. The BCP for the dihydrogen bond shows positive Laplacian indicating a weaker and closed-shell interaction. Moderately large bond ellipticity for the H···H bond indicates the instability involved in the bond. Similar features are also exhibited by the complexes and the corresponding dimers of BH_3H_2O, AlH_3H_2O, and AlH_3NH_3 (cf. Table 3). The $[BH_3H_2O]_2$ has highest ellipticity for the H···H bond among all dihydrogen-bonded dimers. Further, in $[AlH_3NH_3]_2$ one of

TABLE 3: Electron Density Critical Points (CP) and Laplacian of Electron Density of Complexing Molecules, Complexes, and Dimers at the MP2/6-31++G(d,p) Geometry[a]

molecule	location of CP	type of CP	$\rho(r)$	$\nabla^2\rho(r)$	ϵ
LiH	Li−H bond	(3, −1)	0.0355	0.1550	0.000
H_2O	O−H bond	(3, −1)	0.3709	−2.2572	0.027
H_2OLiH (S1)	Li−O bond	(3, −1)	0.0279	0.2238	0.080
	Li−H bond	(3, −1)	0.0352	0.1428	0.002
	O−H bond	(3, −1)	0.3640	−2.3298	0.025
$[H_2OLiH]_2$	Li−O bond	(3, −1)	0.0412	0.3556	0.067
	Li−H bond	(3, −1)	0.0284	0.1315	0.017
	O−H bond (not in H···H)	(3, −1)	0.3645	−2.2274	0.017
	O−H bond (in H···H)	(3, −1)	0.2392	−1.0745	0.021
	H···H bond	(3, −1)	0.0756	−0.0252	0.001
	ring CP	(3, +1)	0.0025	0.0066	
BH_3	B−H bond	(3, −1)	0.1847	−0.2251	0.302
HF	H−F bond	(3, −1)	0.3649	−3.0909	0.000
BH_3HF	B−F bond	(3, −1)	0.0165	0.0632	0.724
	H−F bond	(3, −1)	0.3585	−3.1171	0.001
	B−H bond (out of plane)	(3, −1)	0.1824	−0.2047	0.307
	B−H bond (in plane)	(3, −1)	0.1844	−0.2205	0.295
$[BH_3HF]_2$	B−F bond	(3, −1)	0.0480	0.1067	0.824
	H−F bond	(3, −1)	0.2973	−2.4311	0.004
	B−H bond (not in H···H)	(3, −1)	0.1867	−0.2309	0.227
	B−H bond (not in H···H)	(3, −1)	0.1833	−0.2008	0.253
	B−H bond (in H···H)	(3, −1)	0.1611	−0.0453	0.394
	H···H bond	(3, −1)	0.0412	0.0771	0.158
	ring CP	(3, +1)	0.0056	0.0344	
BH_3H_2O	B−O bond	(3, −1)	0.0597	0.1705	0.263
	B−H bond (in plane)	(3, −1)	0.1720	−0.1159	0.255
	B−H bond (out of plane)	(3, −1)	0.1751	−0.1338	0.237
	O−H bond	(3, −1)	0.3636	−2.3492	0.021
$[BH_3H_2O]_2$	B−O bond	(3, −1)	0.0805	0.5722	0.128
	B−H bond (in H···H)	(3, −1)	0.1600	−0.0249	0.275
	B−H bond (not in H···H)	(3, −1)	0.1725	−0.1080	0.207
	O−H bond (in H···H)	(3, −1)	0.3359	−2.2657	0.019
	O−H bond (not in H···H)	(3, −1)	0.3626	−2.3518	0.019
	H···H bond	(3, −1)	0.0274	0.0673	0.255
	ring CP	(3, +1)	0.0058	0.0312	
AlH_3	Al−H bond	(3, −1)	0.0805	0.2920	0.025
AlH_3H_2O	Al−O bond	(3, −1)	0.0339	0.2341	0.047
	Al−H bond (in plane)	(3, −1)	0.0765	0.2828	0.002
	Al−H bond(out of plane)	(3, −1)	0.0777	0.2870	0.005
	O−H bond	(3, −1)	0.3606	−2.3354	0.023
$[AlH_3H_2O]_2$	Al−O bond	(3, −1)	0.0447	0.3344	0.044
	Al−H bond (not in H···H)	(3, −1)	0.0790	0.2905	0.008
	Al−H bond (in H···H)	(3, −1)	0.0676	0.2597	0.018
	O−H bond (not in H···H)	(3, −1)	0.3588	−2.3149	0.021
	O−H bond (in H···H)	(3, −1)	0.3141	−2.0318	0.021
	H···H bond	(3, −1)	0.0385	0.0585	0.054
	ring CP	(3, −1)	0.0034	0.0164	
NH_3	N−H bond	(3, −1)	0.3497	−1.8880	0.047
AlH_3NH_3	Al−N bond	(3, −1)	0.0422	0.2552	0.000
	Al−H bond (in plane)	(3, −1)	0.0758	0.2818	0.003
	Al−H bond(out of plane)	(3, −1)	0.0758	0.2818	0.003
	N−H bond (in plane)	(3, −1)	0.3457	−1.9147	0.028
	N−H bond (out of plane)	(3, −1)	0.3458	−1.9150	0.028
$[AlH_3NH_3]_2$	Al−N bond	(3, −1)	0.0474	0.2872	0.008
	Al−N bond	(3, −1)	0.0478	0.2909	0.009
	Al−H bond (in H···H)	(3, −1)	0.0722	0.2739	0.008
	Al−H bond (in H···H)	(3, −1)	0.0709	0.2718	0.004
	Al−H bond (not in H···H)	(3, −1)	0.0772	0.2864	0.001
	Al−H bond (not in H···H)	(3, −1)	0.0751	0.2798	0.007
	Al−H bond (not in H···H)	(3, −1)	0.0769	0.2854	0.002
	Al−H bond (not in H···H)	(3, −1)	0.0765	0.2838	0.003
	N−H (in H···H)	(3, −1)	0.3348	−1.8745	0.023
	N−H (in H···H)	(3, −1)	0.3378	−1.8922	0.023
	N−H (not in H···H)	(3, −1)	0.3345	−1.9015	0.026
	N−H (not in H···H)	(3, −1)	0.3341	−1.9056	0.025
	H···H bond	(3, −1)	0.0191	0.0433	0.035
	H···H bond	(3, −1)	0.0160	0.0401	0.104
	Ring CP	(3, +1)	0.0023	0.0097	

[a] For notation of type of CP, see ref 15.

the H···H bonds shows higher ellipticity and less ED indicating it to be a weaker bond than the other. A clear trend is observed in the strength of the dihydrogen bond formed in the dimers from the ED value at the BCP, viz., $[BH_3HF]_2 > [AlH_3H_2O]_2$

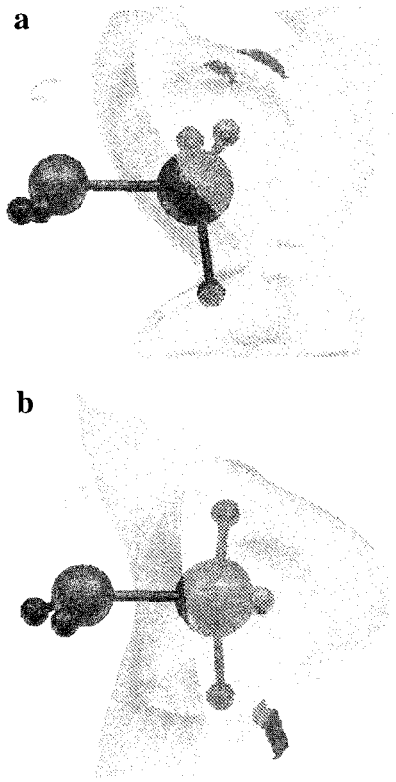

Figure 4. Molecular electrostatic potential isosurfaces of AlH_3H_2O complex: (a) in equilibrium geometry showing isosurfaces of value −12.55 kcal/mol (light) and −27.61 kcal/mol (dark); (b) in dimer geometry showing isosurfaces of values −3.14 kcal/mol (light) and −35.14 kcal/mol (dark).

> $[BH_3H_2O]_2$ > $[AlH_3NH_3]_2$. However, this trend is not reflected in the interaction energies of these dimers (cf. Table 2). This may be attributed to the fact that the geometrical distortions observed in dimers compared to that in their monomers have played a vital role in their stability apart from the dihydrogen bonding.

The molecular electrostatic potential (MESP) maps have been utilized for understanding the reactivity patterns[20] of a molecule. The MESP is defined as

$$V(\mathbf{r}) = \sum Z_A/|\mathbf{r} - \mathbf{R}_A| - \int \rho(\mathbf{r}')/|\mathbf{r} - \mathbf{r}'|\, d^3\mathbf{r}'$$

The MESP is positive around the nuclei and is negative in the region where electrons are localized in the molecule. The regions of electron localization via MESP provide us vital information for rationalizing the structure of weakly bonded and hydrogen-bonded systems.[21] In the present study, we compare the MESP maps of the complexes in their equilibrium and in the dimer geometry for understanding the reasons of structural changes in the dimer formation. The MESP map of H_2OLiH complex in the equilibrium geometry (not presented owing to paucity of space) shows that the MESP surface (−81.58 kcal/mol) lies along the symmetry axis, whereas it exists around the Li−H bond beyond the hydrogen in the dimer geometry. This surface encompasses a larger area in the dimer geometry than in the complex. This is clearly favorable for dimer formation with H···H bonding. The MESP maps of AlH_3H_2O in the equilibrium and in the dimer geometry presented in Figure 4 bring out the utility of this approach. Although there are no significant geometrical distortions in the dimer geometry, one can easily observe a buildup of negative potential around one of the hydrogens attached to Al. This MESP surface has deepened from −27.61 to −35.14 kcal/mol in the dimer geometry. Further, the oxygen lone pair minimum has become shallow in the dimer geometry (−3.14 kcal/mol) compared to that in the equilibrium geometry (−12.55 kcal/mol). This clearly explains the fact that the hydride can attract the acidic hydrogen in H_2O more effectively and the repulsion due to lone pair has also been reduced by small changes in the dimer geometry. Similar features have been observed in the MESP isosurfaces of other complexes in their equilibrium and the dimer geometries. Thus, it may be concluded that the geometrical changes in the complex while forming the dimer occur so as to increase the electrostatic interactions. To confirm this, the results of energy decomposition analysis for dimers are presented in the next section.

TABLE 4: Energy Decomposition Analysis[a] of Interaction Energies of Dihydrogen-Bonded Complexes and Dimers of Complexes[b]

molecule (structure)	ES	EX	PL	CT	MIX	total
$[H_2OLiH]_2$ (S_4)	−81.40	94.02	−26.80	−125.30	89.15	−50.33
$[BH_3H_2O]_2$ (S_{15})	−25.02	24.49	−9.37	−9.97	6.97	−13.09
$[BH_3HF]_2$ (S_{11})	−23.01	33.19	−12.83	−17.83	7.27	−13.21
$[AlH_3NH_3]_2$ (S_{25})	−18.40	14.71	−5.82	−5.55	5.05	−10.01
$[AlH_3H_2O]_2$ (S_{20})	−32.42	35.62	−12.46	−18.94	10.05	−18.14
H_2OLiH (S_2)	−50.51	50.34	−46.78	−41.06	69.82	−17.69
H_2OLiH (S_3)	−8.59	4.75	−1.62	−0.96	1.36	−5.05
BH_3HF (S_9)	−0.92	1.11	−0.67	−0.42	0.29	−0.61
BH_3HF (S_{10})	−1.49	1.62	−0.57	−0.70	0.34	−0.80
BH_3H_2O (S_{14})	−0.55	0.55	−0.15	−0.15	−0.02	−0.32
H_2SLiH	−7.49	7.94	−2.75	−4.09	3.28	−3.11

[a] For details of energy decomposition analysis, see ref 11. The MP2-optimized geometries are used for the analysis. [b] All values are in kcal/mol.

V. Energy Decomposition Analysis

The energy decomposition analysis (EDA) due to Kitaura and Morokuma[11] provides details of contribution to the interaction energy from various components, such as electrostatic (ES), polarization (PL), exchange (EX), charge transfer (CT), etc. It is known that the conventional hydrogen bonds are stabilized by electrostatic contribution.[22] The analysis is carried out for some dihydrogen-bonded complexes and dimers at their MP2-optimized geometries, and details are provided in Table 4. It can be observed from Table 4 that the electrostatic contribution is the largest followed by charge transfer and polarization for all dihydrogen-bonded dimers. The only exception is seen in the case of $[H_2OLiH]_2$, wherein the charge transfer exceeds the electrostatic contribution. In general for dimers, the ES is comparable in magnitude to the EX. Although all H···H bonded complexes in Table 4 are not minima on the PES, we have performed EDA for some such complexes. For these complexes, in general the polarization contribution is larger than the charge transfer. In addition to these complexes, Table 4 reports EDA for the H_2SLiH complex, which exhibits a dihydrogen bond and is a minimum on the MP2 level PES with a stabilization of −3.11 kcal/mol. Analogous to dimers of complexes, the CT contribution is greater than PL for this complex. One may infer from these results that CT is larger than PL for the systems wherein the H···H bonding is the chief cause of stabilization.

VI. Concluding Remarks

A systematic investigation of the dihydrogen bond formed in the molecular systems containing main group elements has

been carried out. The emphasis of this study is to examine the trends found in H···H-bonded complexes and dimers rather than computational results at a high level of theory. In the complexes of LiH, BH_3, and AlH_3 with HF, H_2O, and NH_3, the dihydrogen-bonded structures are not found to be stable. However, the dimers of some of the complexes are formed in a head-to-tail manner and indeed exhibit the dihydrogen bonding. Although the dimer structures of BH_3NH_3 and AlH_3NH_3 have already been reported, the other dimer structures have so far not been studied. The H···H-bonded dimer structures at the RHF level have longer dihydrogen bonds compared to the MP2 ones. Owing to inclusion of correlation, the dimers are found to form a compact structure. The angle (X)−H···H−E (where X = F/O/N and E = Li/B/Al) in the dimers is found to be strongly bent. The bend in the H···H bond decreases as the electronegativity of the proton-donating group increases. On the other hand, the angle X−H···H(E) lies in the range of conventional hydrogen bond (160−180°). Further, for the dimers of complexes of BH_3 and AlH_3, the energy associated with the dihydrogen bond is found to be similar to the conventional moderate or weak hydrogen bond, whereas for the $[H_2OLiH]_2$ it is in the range of the strong hydrogen bond.[13] The dimerization energies at the CCSD(T) indicate that the RHF level values are underestimated whereas the MP2 ones are overestimated. The similarity in the trends of dimerization energies and dipole moment data of the dimerizing complexes indicate that dimerization is dipole-controlled. Moreover, a clear-cut trend is observed in the bond strength of the dihydrogen bond from the ED values at the BCP. The decomposition analysis of interaction energies indicates that, analogous to the conventional hydrogen bond, the H···H bond is predominantly electrostatic in nature and the order ES > CT > PL is generally followed. The notable exception is found in the $[H_2OLiH]_2$, which shows charge transfer as a chief cause of stabilization. For the dimers, the total interaction energy is 0.52 to 0.62 times the corresponding ES contribution.

These conclusions may prove vital in the synthesis of novel structures analogous to those recently reported[23] $[(GaH_2NH_2)_3]_2$. This dimer is believed to be stabilized by dihydrogen bonding. Similar examples of dihydrogen bonding may be obtained from the trimers of BH_3 with H_2O and HF and AlH_3 with H_2O. The dimer structures reported herein may serve as a crucial starting point in this direction.

Acknowledgment. The author acknowledges financial assistance from University Grants Commission (UGC) in the form of a minor research grant and Council of Scientific and Industrial Research (CSIR) [01(1380)/95/EMR-II]. Thanks are also due to Dr. J. J. P. Stewart and Professor S. R. Gadre for helpful discussions and Mr. Alok Srivastava for computational assistance.

References and Notes

(1) Crabtree, R. H.; Siegbahn, P. E. M.; Eisenstein, O.; Rheingold, A. L.; Koetzle, T. F. *Acc. Chem. Res.* **1996**, *29*, 348. Richardson, T. B.; deGala, S.; Crabtree, R. H.; Siegbahn, P. E. M. *J. Am. Chem. Soc.* **1995**, *117*, 12875.

(2) Wessel, J.; Lee, J. C., Jr.; Peris, E.; Yap, G. P. A.; Fortin, J. B.; Ricci, J. S.; Sini, G.; Albinati, A.; Koetzle, T. F.; Eisenstein, O. Rheingold, A. L.; Crabtree, R. H. *Angew. Chem., Int. Ed. Engl.* **1995**, *32*, 2507. Belkova, N. V.; Shubina, E. S.; Ionidis, A. V.; Epstein, L. M.; Jacobsen, H.; Messmer, A.; Berke, H. *Inorg. Chem.* **1997**, *36*, 1522.

(3) Lough, A. J.; Park, S.; Ramachandran, R.; Morris, R. H. *J. Am. Chem. Soc*. **1994**, *116*, 8356. Lee, J. C., Jr.; Peris, E.; Rheingold, A. L.; Crabtree, R. H. *J. Am. Chem. Soc*. **1994**, *116*, 11014.

(4) Orlova, G.; Scheiner, S. *J. Phys. Chem*. **1998**, *102*, 260. Peris, E.; Lee, J. C., Jr.; Rambo, J. R.; Eisenstein, O.; Crabtree, R. H. *J. Am. Chem. Soc.* **1995**, *117*, 3485.

(5) Liu, Q.; Hoffmann, R. *J. Am. Chem. Soc*. **1995**, *117*, 10108.

(6) Cramer, C. J.; Gladfelter, W. L. *Inorg. Chem*. **1997**, *36*, 5358.

(7) Schmidt, M. W.; Baldridge, K. K.; Boatz, J. A.; Elbert, S. T.; Gordon, M. S.; Jensen, J. H.; Koseki, S.; Matsunaga, N.; Nguyen, K. A.; Su, S. J.; Windus, T. L.; Dupuis, M.; Montgomery, J. A. GAMESS. *J. Comput. Chem*. **1993**, *14*, 1347−1363.

(8) Jonas, V.; Thiel, W. *J. Chem. Phys*. **1996**, *105*, 3636; **1995**, *102*, 8474.

(9) Frisch, M. J.; Trucks, G. W.; Schlegel, H. B.; Gill, P. M. W.; Johnson, B. G.; Robb, M. A.; Cheeseman, J. R.; Keith, T.; Petersson, G. A.; Montgomery, J. A.; Raghavachari, K.; Al-Laham, M. A.; Zakrzewski, V. G.; Ortiz, J. V.; Foresman, J. B.; Peng, C. Y.; Ayala, P. Y.; Chen, W.; Wong, M. W.; Andres, J. L.; Replogle, E. S.; Gomperts, R.; Martin, R. L.; Fox, D. J.; Binkley, J. S.; Defrees, D. J.; Baker, J.; Stewart, J. J. P.; Head-Gordon, M.; Gonzalez, C. and Pople, J. A. *Gaussian 94*, Revision B.3; Gaussian, Inc., Pittsburgh, PA, 1995.

(10) UNIPROP: program developed by Gadre and co-workers at University of Pune, India. See also: Shirsat, R. N.; Bapat, S. V.; Gadre, S. R. *Chem. Phys. Lett.* **1992**, *200*, 373. Visualization program UNIVIS developed by Gadre and co-workers at University of Pune, India. See also: Limaye, A. C.; Inamdar, P. V.; Dattawadkar, S. M.; Gadre, S. R. *J. Mol. Graphics* **1996**, 14.

(11) Kitaura, K.; Morokuma, K. *Int. J. Quantum Chem*. **1976**, *10*, 325. Morokuma, K.; Kitaura, K. In *Chemical Applications of Electrostatic Potentials*; Politzer, P., Truhlar, D. G., Eds.; Plenum: New York, 1981.

(12) Szczesniak, M. M.; Ratajczak, H. *Chem. Phys. Lett.* **1980**, *74*, 243. Dill, J. D.; Schleyer, P. v. R.; Binkley, J. S.; Pople, J. A. *J. Am. Chem. Soc*. **1977**, *99*, 6159. Atwood, J. L.; Butz, K. W.; Gardiner, M. G.; Jones, C.; Koutsantonis, G. A.; Ratson, C. L.; Robinson, K. D. *Inorg. Chem*. **1993**, *32*, 3482.

(13) Jeffrey, G. A. *An Introduction to Hydrogen Bonding*; Oxford University Press: Oxford, 1997. Wells, A. F. *Structural Inorganic Chemistry*; Oxford University Press: Oxford, 1984.

(14) Boys, S. F.; Bernardi, F. *Mol. Phys.* **1970**, *19*, 553.

(15) Bader, R. F. W. *Atoms in Molecules: A Quantum Theory*; Clarendon: Oxford, 1990. The critical points of molecular electron density distribution (ED) can be characterized from its rank and signature (excess of positive eigenvalues over negative ones). Thus, maxima are denoted as (3, −3), minima are denoted as (3, +3), and two types of saddles are denoted as (3, −1) and (3, +1). The ED is maximum at the nuclear sites, and a (3, −1) saddle is found between every bonded pair of atoms (called the bond critical point). The presence of ring or cage in the system can be identified from occurrence of the (3, +1) saddle and minimum, respectively, in the ED distribution.

(16) Bone, R. G. A.; Bader, R. F. W. *J. Phys. Chem*. **1996**, *100*, 10892. Bader, R. F. W.; Essen, H. *J. Chem. Phys*. **1984**, *80*, 1943.

(17) Koch, U.; Popelier, P. L. A. *J. Phys. Chem.* **1995**, *99*, 9747.

(18) Boyd, R. J.; Choi, S. C. *Chem. Phys. Lett.* **1985**, *120*, 80.

(19) Popelier, P. L. A. *J. Phys. Chem*. **1998**, *102*, 1873.

(20) *Chemical Applications of Atomic and Molecular Electrostatic Potentials*; Politzer, P., Truhlar, D. G., Eds.; Plenum: New York, 1981. *Theoretical and Computational Chemistry, Vol. 3—Molecular Electrostatic Potentials: Concepts and Applications*; Murray, J. S., Sen, K. D., Eds.; Elsevier: Amsterdam, 1996. Gadre, S. R.; Kulkarni, S. A.; Shrivastava, I. H. *J. Chem. Phys.* **1992**, *96*, 5253.

(21) Buckingham, A. D.; Fowler, P. W. *J. Chem. Phys.* **1983**, *79*, 6426. Gadre, S. R.; Pundlik, S. S. *J. Phys. Chem*. **1997**, *101*, 3298.

(22) Rendell, A. P. L.; Backsay, G. B.; Hush, N. S. *Chem. Phys. Lett.* **1985**, *117*, 400.

(23) Campbell, J. P.; Hwang, J. W.; Young, V. G., Jr.; Von Dreele, R. B.; Cramer, C. J.; Gladfelter, W. L. *J. Am. Chem. Soc.* **1998**, *120*, 521.